

# Nonuniform Recrystallization in a Mechanically Alloyed Nickel-Base Superalloy

K. MURAKAMI, K. MINO, H. HARADA, and H.K.D.H. BHADESHIA

The recrystallization behavior of mechanically alloyed and extruded MA6000 oxide dispersion strengthened (ODS) nickel-base superalloy has been studied as a function of the position of the sample in the extruded bar. It was found that there are profound differences across the cross section of the bar, the edge regions recrystallizing more easily relative to the core. Furthermore, the recrystallized grains tend to be much more anisotropic at the edges. It appears that these differences are caused by inhomogeneous deformation. The oxide particles are more aligned along the extrusion direction at the regions near the surface, presumably because of the more extensive deformation in those regions. This explains the greater anisotropy in the recrystallized grains and the relative ease of recrystallization (since the boundary mobility along the extrusion direction is high for aligned particles). Stored energy measurements confirm that the observed effects cannot be explained by differences in the driving force for recrystallization.

## I. INTRODUCTION

INCONEL\* MA6000 is a nickel-base superalloy de-

---

\*INCONEL is a trademark of Inco Alloys International, Inc., Huntington, WV.

---

signed for aerospace applications, strengthened with both  $\gamma'$  precipitates and yttria particles.<sup>[1]</sup> It is manufactured by a powder metallurgical process called "mechanical alloying",<sup>[2]</sup> in which elemental powders or compounds are heavily deformed while in intimate contact to such large strains that the mechanical mixture changes into a solid solution, although the yttrium oxide particles do not alloy but form a dispersion which adds to the elevated temperature strength. The alloyed powder is then canned and hot-rolled and/or hot-extruded; the microstructure at this stage consists of incredibly fine ( $\approx 0.4 \mu\text{m}$ ) equiaxed grains resulting from dynamic recrystallization during the hot deformation.<sup>[3]</sup> Subsequent annealing in a temperature gradient yields highly anisotropic grains by a process of secondary recrystallization, giving a grain structure reminiscent of directional solidification. This *directionally recrystallized* microstructure produced by solid-state processing is eminently suited for applications where creep resistance is of paramount importance.

Both the mechanical alloying process and the subsequent hot-deformation processes can lead to inhomogeneities, especially since the strength levels involved even at high temperatures are large. It is common knowledge that such materials tend to show batch-to-batch variations and variations within single extruded samples. The former can be minimized by careful control of the manufacturing process. The purpose of the present work is to examine the secondary recrystallization behavior

across the cross section of extruded bar in order to understand better the factors responsible for variations in grain structure across the cross section. It is unlikely that such variations can be eliminated completely, given the difficulties in processing. Nevertheless, a better understanding of the inhomogeneities that might exist can perhaps suggest heat-treatment procedures which give uniform microstructures in spite of any heterogeneities.

## II. EXPERIMENTAL PROCEDURE

### A. Alloy Composition and Processing

The alloy (Table I) was prepared at Inco Alloys (Hereford, England) by the mechanical-alloying technique. This involves the ball-milling of a mixture of nickel powder (particle size 4 to 7  $\mu\text{m}$ ) and powdered chromium, molybdenum, tungsten, tantalum, and a master nickel-base alloy powder containing the reactive elements aluminum, titanium, boron, and zirconium (particle size  $\approx 150 \mu\text{m}$ ). The yttrium oxide is introduced into the mixture in the form of 1- $\mu\text{m}$  aggregates, each consisting of numerous individual particles of 20 to 40 nm diameter.

The mechanically alloyed powder is then canned in mild steel and extruded into a 48-mm-diameter bar, followed by hot-rolling (1040 °C) into 23-mm square bar. The normal commercial practice at this stage is to induce recrystallization into an anisotropic grain microstructure, but for the present purposes, the alloy was supplied in the as-extruded and rolled state.

### B. Optical Microscopy, Differential Scanning Calorimeter, and Heat Treatment

Metallographic samples (10 × 23 × 23 mm) were prepared on a plane normal to the extrusion (and rolling) direction. They were etched using a mixture of 2 g CuCl<sub>2</sub> in 40 ml HCl and 80 ml ethanol.

The heat treatments were carried out in a differential scanning calorimeter (DSC) which has a computer-controlled furnace, using 5 × 5 × 2 mm samples taken from specific positions within the cross section of the

---

K. MURAKAMI, Researcher, and H. HARADA, Senior Researcher, are with the Research Development Corporation of Japan, Tokyo, Japan. K. MINO, formerly Senior Researcher, Research Development Corporation of Japan, is now Senior Researcher, Ishikawazima-Harima Heavy Industries Co., Ltd., Tokyo, Japan. H.K.D.H. BHADESHIA, Lecturer, is with the Department of Materials Science and Metallurgy, University of Cambridge, Cambridge CB2 3QZ, United Kingdom.

Manuscript submitted February 7, 1992.

**Table I. Chemical Composition of Nickel-Base Superalloy MA6000 (Weight Percent)**

C	Cr	Al	Ti	Ta	Mo
0.058	14.96	4.44	2.28	1.97	1.96
W	Zr	Si	Mn	P	S
3.91	0.13	0.08	0.01	0.006	0.001
Co	Cu	Fe	N	Nb	V
0.22	0.01	1.49	0.20	0.05	0.01
Y <sub>2</sub> O <sub>3</sub>	Ni				
1.08	balance				

bar. One of the long edges of the sample was parallel to the extrusion (and rolling) direction.

Differential scanning calorimetry was carried out using a Netzsch DSC 404/3/413/D machine which is a specially designed high-temperature, heat flux DSC with computer control and data acquisition. It uses a Pt/Rh furnace which has very low-temperature gradient characteristics. The sample and reference are placed in thermally balanced Pt crucibles. A differential signal is generated when an event causes difference in heat evolution or heat capacity between the sample and its reference; this signal can be converted into thermodynamic data associated with the event. Experiments can be carried out to a maximum temperature of about 1500 °C.

Calorimetric measurements were carried out during continuous heating (2.5 to 40 K min<sup>-1</sup>); both the sample mass and reference mass were typically about 200 mg. The reference was made of the same alloy as the sample, but it was in the recrystallized state. This led to a very significant improvement in accuracy when compared with other reference materials, such as pure nickel, consistent with earlier research.<sup>[4]</sup> In all cases, the samples were examined using light microscopy to confirm recrystallization. All the experiments were carried out using an argon atmosphere in the DSC chamber, the argon flow rate being 50 K min<sup>-1</sup>.

"Isothermal annealing" experiments were also carried out in the DSC, involving the heating of samples to the chosen isothermal temperature at a rate of 20 K min<sup>-1</sup> and then holding at the annealing temperature for a variety of time periods. The samples were prepared, as illustrated in Figure 1, from the surface, intermediate, and core regions of the bar.

### III. RESULTS AND DISCUSSION

#### A. Gamma Prime Solution

It is now well established that the onset of recrystallization in mechanically alloyed oxide dispersion strengthened (ODS) superalloys does not correlate with the dissolution of  $\gamma'$  precipitates during heating. Nevertheless, recrystallization always occurs at some temperature beyond that at which the  $\gamma'$  has dissolved. It was therefore intended to conduct the isothermal annealing experiments at temperatures above the  $\gamma'$  solution temperature which was determined experimentally using differential scanning calorimetry.

In order to observe separately the enthalpy changes due to recrystallization and due to  $\gamma'$  solution, the reference was chosen to be an already recrystallized MA6000

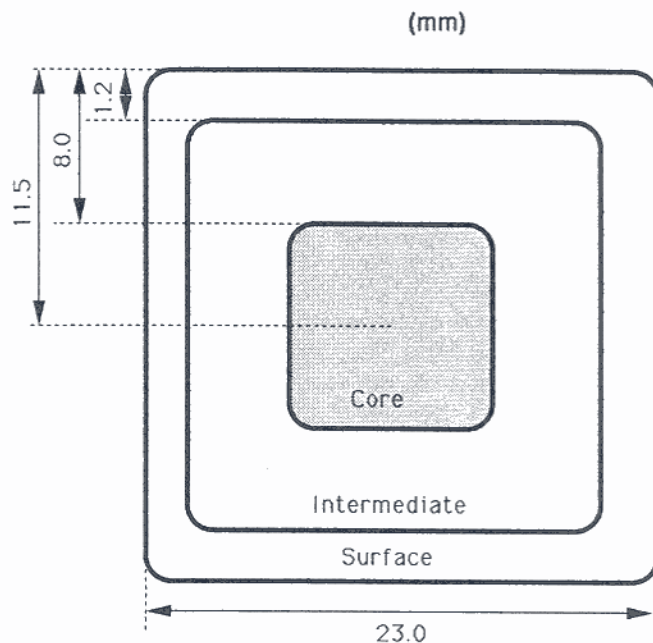


Fig. 1—Illustration of the surface, intermediate, and core samples extracted from extruded MA6000 bar. The extrusion direction is normal to the plane of the diagram.

specimen. If the sample and reference masses are exactly identical, and if their  $\gamma'$  solution kinetics are also identical, then a DSC experiment would not register any effect due to  $\gamma'$ . Such circumstances are, however, extremely unlikely. The  $\gamma'$  solution is endothermic during heating, whereas recrystallization is exothermic. Hence, by ensuring that the reference has a slightly smaller mass than the sample, it is possible to ensure that the two peaks due to  $\gamma'$  solution and recrystallization point in opposite directions.

Figure 2 shows a typical experimental result which indicates that most of the  $\gamma'$  is in solution by about 1180 °C at a heating rate of 10 K min<sup>-1</sup>. The recrystallization and solution processes are seen to be well separated in terms of temperature. Figure 3 illustrates further data; as expected, the solution kinetics are elevated to



Fig. 2—Typical differential calorimetric curve illustrating the  $\gamma'$  is dissolution and recrystallization peaks. The heating rate is 10 K min<sup>-1</sup>, the sample is from the intermediate region of the extruded bar, and the reference is a recrystallized sample of slightly smaller mass.

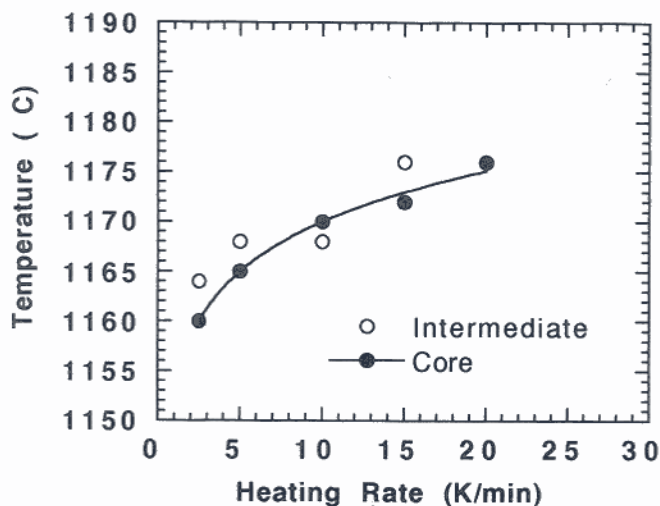


Fig. 3—Differential scanning calorimetry data showing the  $\gamma'$  dissolution start and finish temperatures as a function of heating rate for both intermediate and core samples.

higher temperatures as the heating rate is increased. More significantly, there is no dependence of  $\gamma'$  solution kinetics on sample position within the bar. This indicates that any inhomogeneous recrystallization behavior cannot be attributed to variations in chemistry or  $\gamma'$  morphology with position.

As already pointed out, isothermal annealing was achieved by heating the samples to the chosen temperature at a rate of  $20 \text{ K min}^{-1}$ . Figure 3 indicates that for  $20 \text{ K min}^{-1}$ , the  $\gamma'$  should be dissolved by  $1180^\circ\text{C}$ . All isothermal annealing experiments were therefore carried out above  $1180^\circ\text{C}$ .

### B. Recrystallization during Isothermal Annealing

As pointed out earlier, during solid-state processing, directional grain structures are usually produced by annealing bars in a temperature gradient or by zone annealing. Without this procedure, recrystallization occurs into an equiaxed grain structure; an exception to this is the case where the alloy contains dispersions of particles aligned along the extrusion direction, in which case anisotropic grains are obtained even during isothermal recrystallization.<sup>[5,6]</sup> Thus, isothermal annealing experiments reported below constitute a critical test for the presence or absence of aligned particle dispersions.

The metallographic results following annealing at temperatures in the range  $1180$  to  $1240^\circ\text{C}$  for 60 minutes are presented in Figure 4 and for 1440 minutes in Figure 5. The complete set of results is summarized in Table II.

Samples taken from the surface of the bar (*i.e.*, from a depth not exceeding  $1.2 \text{ mm}$ ) recrystallized most easily, giving extremely anisotropic grains elongated along the extrusion direction. The length-to-width ratio (the aspect ratio), as observed on random sections containing the extrusion direction, was measured to be about 15. The lowest temperature at which recrystallization began was found to be about  $1180^\circ\text{C}$ .

Similar though somewhat retarded recrystallization

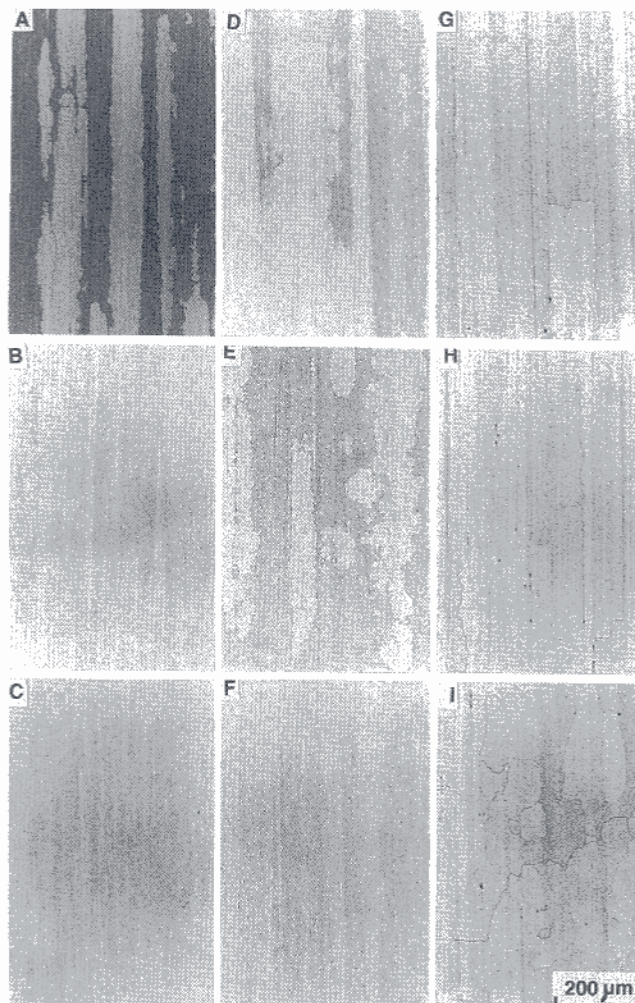


Fig. 4—Metallographic data from annealing experiments carried out at a variety of temperatures for a time period of 60 min: (A) through (C)  $1180^\circ\text{C}$ ; (D) through (F)  $1200^\circ\text{C}$ ; (G) through (I)  $1240^\circ\text{C}$ . (A), (D), and (G) surface; (B), (E), and (H) intermediate; and (C), (F), and (I) core.

behavior was observed in the intermediate regions, where recrystallization occurred during annealing at temperatures below about  $1200^\circ\text{C}$ . The aspect ratio of the anisotropic recrystallized grains was once again measured to be greater than  $\approx 15$ .

Recrystallization was most sluggish in the core regions (depth of greater than  $8 \text{ mm}$  below the surface). Complete recrystallization could only be obtained during annealing at  $1240^\circ\text{C}$ , and the resulting grain structure tended to be more equiaxed with a much smaller aspect ratio of about 4.5.

The development of anisotropic grains during isothermal annealing is attributed to the alignment of oxide particles along the extrusion direction. The alignment is expected to be strongest along the surface regions where the deformation imparted during extrusion is also expected to be most intense.

### C. Stored Energy Measurements

If the degree of deformation is expected to be larger at the surface regions of the bar, then it is possible that

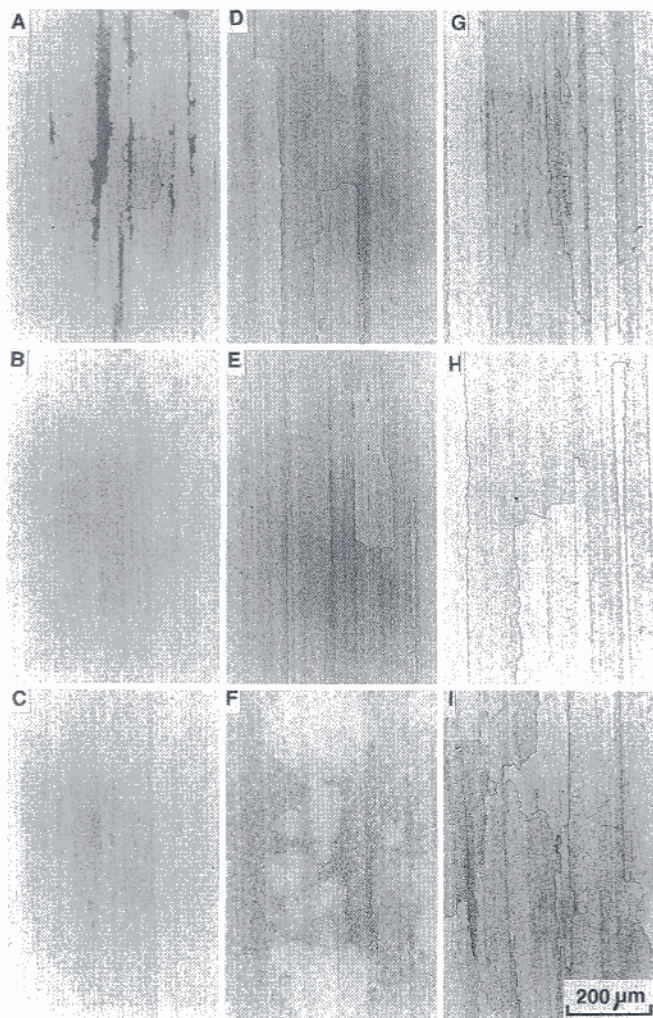


Fig. 5—Metallographic data from annealing experiments carried out at a variety of temperatures for a time period of 1140 min.: (A) through (C) 1180 °C; (D) through (F) 1200 °C; and (G) through (I) 1240 °C. (A), (D), and (G) surface; (B), (E), and (H) intermediate; and (C), (F), and (I) core.

the stored energy in those regions might also be larger. However, it is also possible that the stored energy reaches saturation, in which case it may not vary with position.

Figure 6 shows measurements of the stored energy as a function of the sample position and the heating rate in the DSC. It is evident that there are no significant variations either with position in the extruded bar or with the heating rate. Since almost all of the stored energy in as-extruded MA6000 is in the form of grain boundaries (the grain size is typically of the order of 0.4  $\mu\text{m}$ ), the

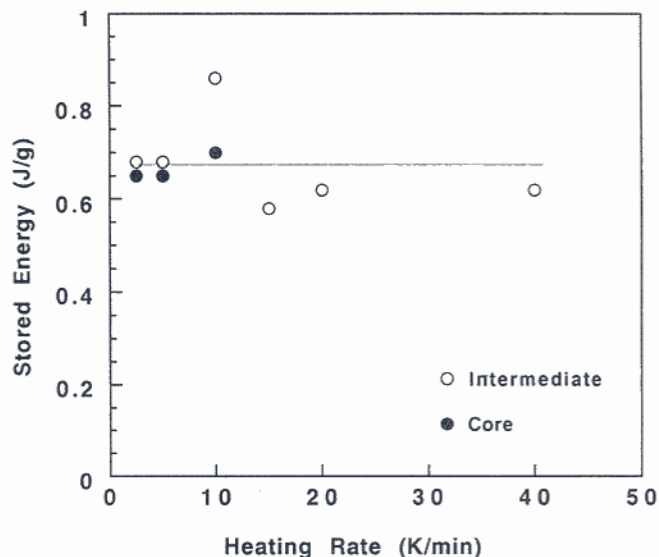


Fig. 6—Variation in stored energy as a function of heating rate and sample position in the extruded bar.

results indicate that there is no difference in the primary grain structure across the cross section of the bars.

Figure 7 illustrates typical DSC curves ( $5 \text{ K min}^{-1}$ ), showing the exothermic recrystallization peaks for both the intermediate and core samples. Although the peak areas are similar, there are clear differences in detail. The intermediate sample begins and completes recrystallization at lower temperatures relative to the core sample. This is consistent with the metallographic data reported earlier from isothermal annealing experiments, that recrystallization is easier for the intermediate samples.

Further experiments involving continuous heating (Figure 8) revealed the same result, that the surface regions always recrystallized more readily relative to the core regions. The core regions were also found to be much more sensitive to the heating rate. The grain microstructures are illustrated in Figure 9; they were found to be anisotropic, although the aspect ratios could not be measured because of the small size of the samples used in the DSC experiments. However, the core grains were always much coarser (Figure 10), their size decreasing as the heating rate increased. This can be expected because recrystallization is delayed to higher temperatures as the heating rate increases, so that the nucleation rate might also be larger. On the other hand, the grain width for the intermediate regions was wholly insensitive to the heating rate, perhaps because the aligned oxide particles prevent growth beyond some limiting size determined by the spacing between the bands of particles.

Table II. Summary of Metallographic Data Following Isothermal Annealing

Time (Min)	60			480			1440		
	Surface	Intermediate	Core	Surface	Intermediate	Core	Surface	Intermediate	Core
1180	●	×	×	●	×	×	●	×	×
1200	○	×	×	○	●	×	○	○	●
1240	○	○	○	○	○	○	○	○	○

○—Complete recrystallization; ●—partial recrystallization; and ×—no recrystallization.

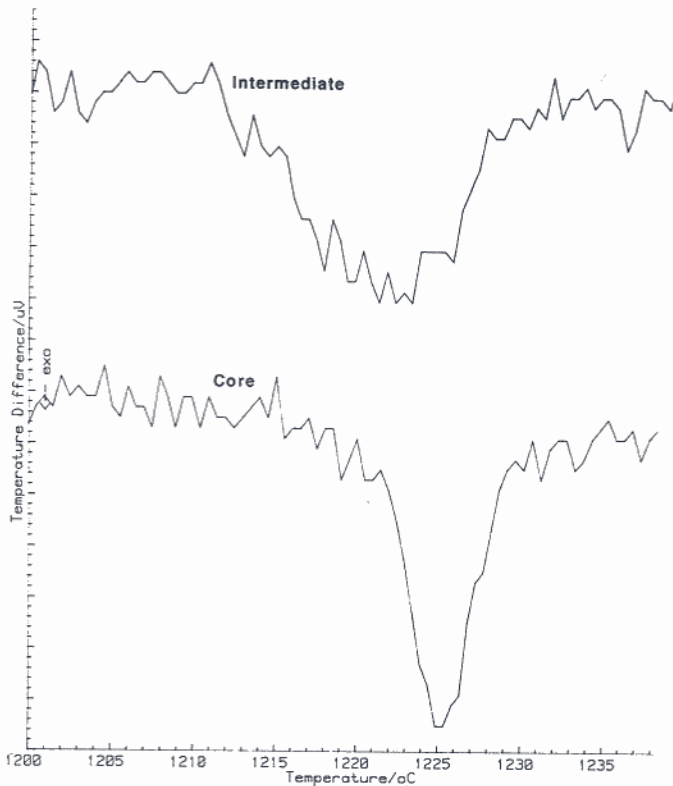


Fig. 7—Typical DSC recrystallization peaks from intermediate and core samples (5 K min<sup>-1</sup>).

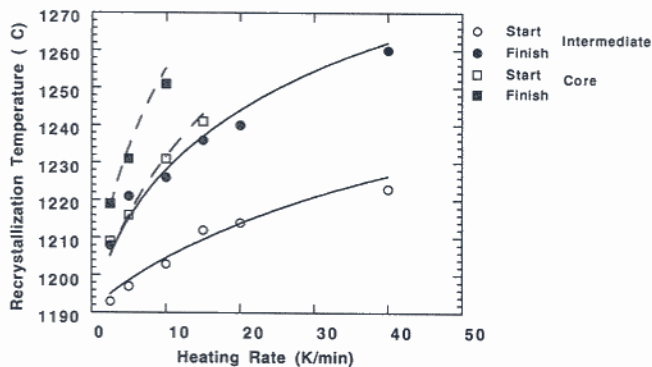


Fig. 8—Recrystallization start and finish temperatures as a function of heating rate and sample position in the extruded bar.

An explanation for these results relies on the earlier hypothesis that the oxide particles are more aligned near the surface regions. For randomly dispersed particles, the grain boundary velocity  $v_R$  is expected to be isotropic. For aligned particles, it should be easier for grain boundary motion to occur parallel to the extrusion direction (velocity  $v_X$ ) and more difficult for motion normal to the extrusion direction  $v_{Y,Z}$ , with  $v_{Y,Z} < v_R < v_X$ . Since growth along the extrusion direction is less impeded, recrystallization can initiate more readily, thereby explaining the faster kinetics at the surface regions.

Figure 11 illustrates some direct evidence for the presence of a higher degree of particle alignment along the extrusion direction in regions close to the surface of the

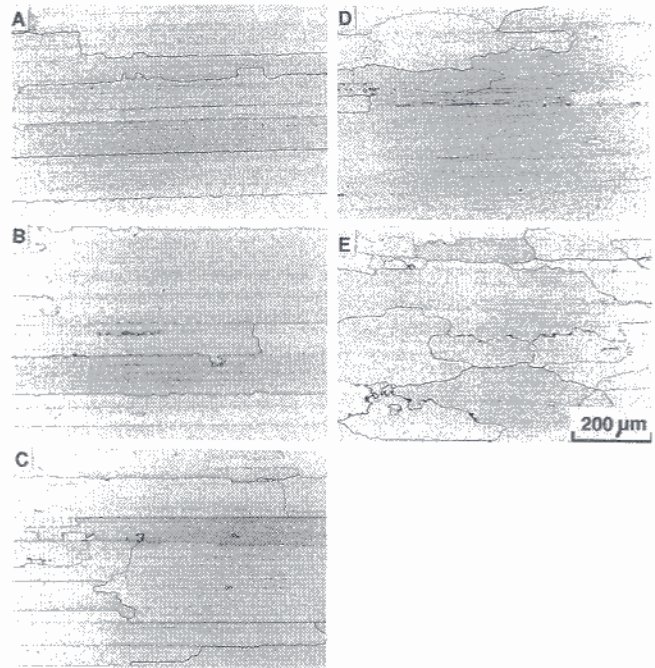


Fig. 9—Metallographic data from continuous heating experiments: (a) and (d) 2.5 K/min; (b) and (e) 10 K/min; and (c) 40 K/min. (a) through (c) intermediate; and (d) and (e) core.

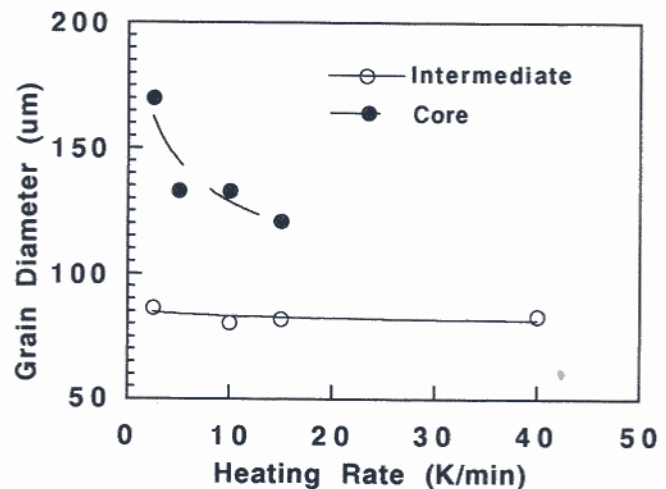


Fig. 10—Plot of the recrystallized grain width as a function of the heating rate and sample position in the extruded bar.

bar. The optical micrographs were obtained by etching in a  $\text{CuCl}_2/\text{HCl}/\text{ethanol}$  mixture, so that the apparent particle size is probably exaggerated.

#### D. Model

The complexity of recrystallization in ODS materials has been emphasized in an excellent review by Humphreys.<sup>[7,8]</sup> The kinetics depend on particle size and dispersion geometry and can be accelerated or retarded depending on the detailed state of the dispersion and the extent of deformation. It is also well established that particles can exert pinning forces on moving grain boundaries.<sup>[9-12]</sup> The work presented subsequently is necessarily

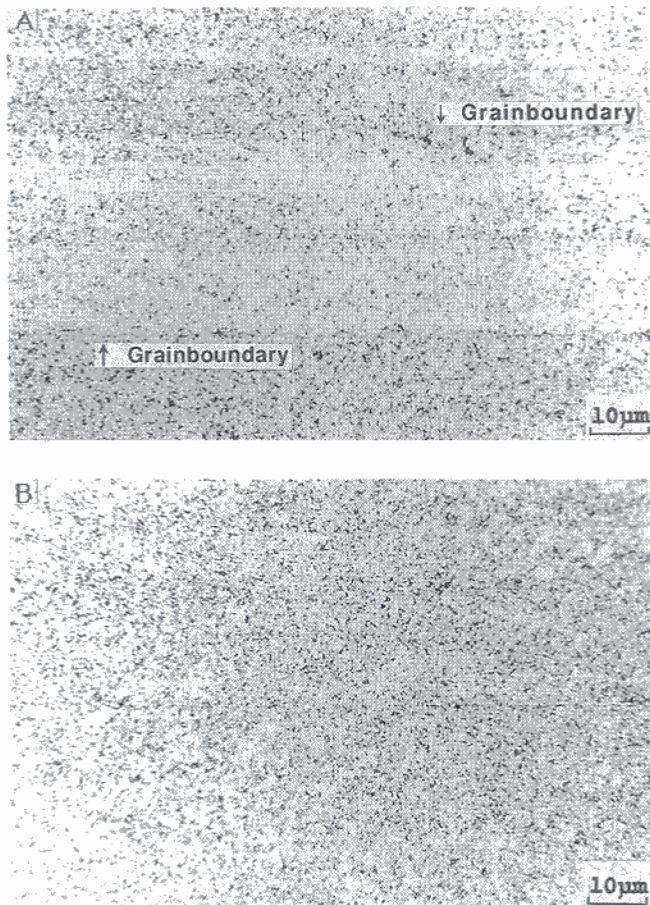


Fig. 11—Optical micrographs from the (A) intermediate and (B) core regions of the extruded bar, illustrating the larger degree of particle alignment associated with the intermediate regions. The extrusion direction is horizontal in each case.

an oversimplification of these complex phenomena, but we believe it is capable of fairly representing the experimental observations.

Two interesting qualitative conclusions emerge from the preceding study: recrystallization is easier in the surface regions and is also less sensitive to the heating rate. Both of these effects were attributed to the relatively larger degree of particle alignment in the surface regions. In this section, we develop a quantitative model which provides further justification for this interpretation of the experimental data.

If it is assumed that the oxide particles all have an identical radius  $r$ , then the number of particles per unit volume is given by

$$N_v = \frac{3V_v}{4\pi r^3} \quad [1]$$

where  $V_v$  is the volume fraction of oxide particles. The particle spacing along the orthogonal directions  $d_x$  (the extrusion direction),  $d_y$ , and  $d_z$  is therefore given by

$$d_x = (A^2/N_v)^{1/3} \quad [2]$$

$$d_y = d_z = d_x/A \quad [3]$$

where  $A$  represents the anisotropy of the oxide particle

dispersion. A value of unity gives an isotropic dispersion, whereas larger values tend to make the particles align along the extrusion direction. It is assumed that the particle spacing is uniform in the directions normal to the extrusion direction. It also follows that the number of particles per unit area is given by

$$N_x = (d_y d_z)^{-1} \quad [4]$$

$$N_y = N_z = (d_x d_z)^{-1} \quad [5]$$

where  $N_x$  is the number density of particles on the plane normal to the  $X$  direction.

The grain boundary velocity during recrystallization is given by<sup>[13]</sup>

$$v = \delta \nu \exp\{-Q/RT\} [1 - \exp\{-\Delta G/RT\}] \quad [6]$$

where  $\delta$  and  $\nu$  are the distance and atomic jump frequency across the boundary, respectively,  $R$  is the universal gas constant, and  $Q$  is an activation energy for the transfer of atoms across the boundary. The term  $\Delta G$  is the effective driving force for recrystallization, which does not vary with temperature but is modified by the particle pinning force:

$$\Delta G \approx \Delta G_s - (C_1 V_v V_M \sigma / r) \quad [7]$$

where  $\Delta G_s$  is the stored energy in the material,  $\sigma$  is the grain boundary energy per unit area, and  $V_M \approx 7.1 \times 10^{-6} \text{ m}^3 \text{ mol}^{-1}$  is the molar volume. The term  $C_1$  is a constant whose magnitude depends on the details of the pinning process.<sup>[9]</sup> The equation applies to the case where the particles are uniformly dispersed. When they are not, we get

$$\Delta G_{x,y,z} \approx \Delta G_s - (C_1 r N_{x,y,z} V_M \sigma) \quad [8]$$

making the boundary velocity a function of the orientation relative to the extrusion direction.

It is reasonable to assume that recrystallization begins from a number of pre-existing nuclei, so that the fraction  $\xi$  of the sample that is isothermally recrystallized can be obtained using the classic Johnson-Mehl-Avrami<sup>[14]</sup> approach as

$$\xi = 1 - \exp\{-n_v \nu_x \nu_y \nu_z t^3\} \quad [9]$$

where  $n_v$  is the fixed number of nuclei available per unit volume at the start of recrystallization and  $t$  is the heat-treatment time.

The theory presented so far deals with isothermal recrystallization; the experiments, on the other hand, involved continuous heating. This anisothermal heat treatment can be taken into account by representing the continuous heating curve as a series of small isothermal steps at successively rising temperatures. Each step thus represents an isothermal anneal for a time period  $t_i$ , where the subscript denotes the step number. The value of the fraction recrystallized, the time interval, and the temperature for the first step are, therefore,  $\xi_1$ ,  $t_1$ , and  $T_1$ , respectively. To achieve this same degree of transformation, but at the temperature  $T_2$ , requires, in general, a different time  $t'_1$ . Assuming that the reaction is isokinetic,<sup>[14]</sup> the value of  $\xi_2$  can be estimated by annealing for a time interval  $t'_1 + t_2$  at  $T_2$ . This procedure can be continued until the sample is fully recrystallized.

The calculations were carried out assuming the values

**Table III. Parameters Used in the Model for Recrystallization in the Presence of an Anisotropic Dispersion of Oxide Particles**

$Q$	$284,512 \text{ J mol}^{-1}$
$\sigma$	$0.6 \text{ J m}^{-2}$
$V_v$	0.01
$r$	$1 \times 10^{-8} \text{ m}$
$\Delta G_s$	$30 \text{ J mol}^{-1}$
$\delta v$	$1.5 \times 10^{10} \text{ m min}^{-1}$
$n_v$	$7.4 \times 10^8 \text{ m}^{-3}$

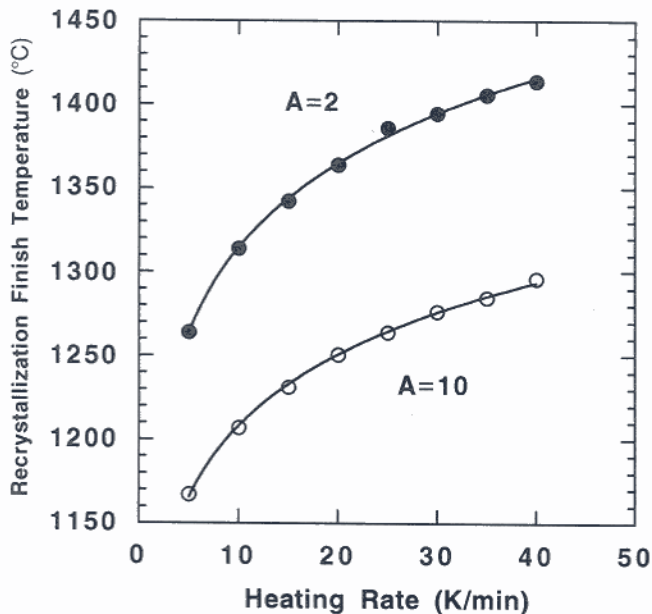


Fig. 12—Calculations illustrating the variation in the recrystallization finish temperature as a function of the heating rate and of the degree of anisotropy ( $A$ ) in the oxide dispersion. A more uniform oxide dispersion leads to a higher recrystallization temperature and a larger sensitivity to the heating rate.

listed in Table III. Most of these values are crude (though reasonable) estimates, so that the results from the model should only be used to assess trends rather than give exact agreement with experimental data. It has been verified that the trends are not sensitive to the chosen values of the input parameters. The activation energy  $Q$  is assumed to be that for the self diffusion of nickel,<sup>[15]</sup> and  $C_1$  is chosen in order to obtain recrystallization at temperatures close to those observed.

Calculations using the model and the parameters listed in Table III are presented in Figure 12. They confirm that recrystallization can be expected to occur at higher temperatures as the precipitate dispersion becomes more uniform. Furthermore, the recrystallization kinetics also should become more sensitive to the heating rate (for samples with relatively uniform dispersions), consistent with experimental observations.

## IV. CONCLUSIONS

Extruded bars of MA6000 mechanically alloyed, ODS nickel-base superalloy are found to exhibit significant variations in microstructure following secondary recrystallization anneals. The surface regions are found to recrystallize at a more rapid rate relative to the cores of the bars. Furthermore, the recrystallized grains at the surface are more anisotropic relative to the core regions. These results can be understood if it is assumed that inhomogeneous deformation during extrusion causes a more pronounced alignment of oxide particles at the surface regions. This interpretation has, to some extent, been verified using a theoretical model for recrystallization in the presence of an anisotropic dispersion of pinning particles.

## ACKNOWLEDGMENTS

The authors are grateful to Professor C.J. Humphreys for the provision of laboratory facilities at the University of Cambridge and to Dr. M. Yamazaki for his help in facilitating this project. This work was carried out under the auspices of the "Atomic Arrangements: Design and Control Project," which is a collaborative effort between the University of Cambridge and the Research and Development Corporation of Japan. The alloy used was kindly supplied by Dr. Ian Elliott of Inco Alloys (Hereford).

## REFERENCES

1. G.A.J. Hack: *Powder Metall.*, 1984, vol. 27, p. 73.
2. John S. Benjamin: *Metall. Trans.*, 1970, vol. 1, p. 2943.
3. M. Baloch and H.K.D.H. Bhadeshia: *Mater. Sci. Technol.*, 1990, vol. 6, p. 1236.
4. K. Mino, H. Harada, H.K.D.H. Bhadeshia, and M. Yamazaki: *Mater. Sci. Forum*, 1992, vols. 88–90, pp. 213–20.
5. M. Baloch: Ph.D. Thesis, University of Cambridge, Cambridge, United Kingdom, 1989.
6. N. Deards and H.K.D.H. Bhadeshia: *Mater. Sci. Forum*, 1992, vols. 94–96, pp. 741–46.
7. F.J. Humphreys: *Met. Sci.*, 1979, vol. 13, p. 136.
8. F.J. Humphreys: *Recrystallization '90*, T. Chandra, ed., TMS, Warrendale, PA, 1990, p. 113.
9. C. Zener: Private communication to C.S. Smith, *Trans. TMS-AIME*, 1949, vol. 175, p. 15.
10. E. Nes, N. Ryum, and O. Hundri: *Acta Metall.*, 1985, vol. 33, p. 11.
11. O. Hundri, E. Nes, and N. Ryum: *Acta Metall.*, 1989, vol. 37, p. 129.
12. M.F. Ashby, J. Harper, and J. Lewis: *Trans. TMS-AIME*, 1969, vol. 245, p. 413.
13. J.W. Christian: *Theory of Transformations in Metals and Alloys*, Part I, 2nd ed., Pergamon Press, Oxford, United Kingdom, 1975, p. 479.
14. J.W. Christian: *Theory of Transformations in Metals and Alloys*, Part I, 2nd ed., Pergamon Press, Oxford, United Kingdom, 1975, p. 545.
15. *Handbook of Chemistry and Physics*, 57 ed., R.C. Weast, ed., CRC Press, Cleveland, OH, 1977.